Perturbations of an anisotropic spacetime: Dust filled medium

Hyerim Noh
Korea Astronomy Observatory, San 36-1, Whaam-dong, Yusung-gu, Daejon, Korea
(Received 21 November 1995)

We investigate the evolution of a perturbed Bianchi type-I universe filled with a (pressureless) dust medium. The background model shows a smooth transition from the early shear-dominated anisotropic stage to the dust-dominated isotropic stage. We have exact solutions describing the background evolution. We consider the situations where the perturbation wave vector lies in a plane made of two principal axes of the background anisotropy. We take the comoving gauge. We numerically investigate the behavior of perturbation as it goes through the transition. The results show that in the shear-dominated stage the density perturbation shows the coupling with the gravitational wave perturbations. Because of the coupling the density perturbation in the small scale shows an oscillatory behavior with a decreasing amplitude.

PACS number(s): 98.80.Hw, 95.30.Sf

I. INTRODUCTION

We have been investigating the evolution of perturbations in a Bianchi type-I universe model. In [1] we presented a formulation which can be applied to a general system made of fluids or fields. In [2] we considered the case where the energy-momentum content consists of an ideal fluid with a vanishing entropic and anisotropic pressure. As a specific example of the ideal fluid situation, in [3] we investigated the case with the radiation fluid where $w \equiv p/\mu = \frac{1}{3}$; p and μ are the pressure and the energy density, respectively. We have the radiation-dominated stage preceding the dust-dominated stage of the present universe. For $w = \frac{1}{3}$ the exact solutions for the evolution of the background anisotropic model are known in analytic forms. These analytic solutions for the background evolution are not necessary for a numerical investigation, but provide the clearer interpretation of results.

In this paper we investigate the case where the energy-momentum content consists of a pressureless dust. The dust fluid can be considered as a case of the ideal fluid with $w = 0$. In this case we also have exact solutions for the background evolution. The early shear-dominated anisotropic stage shows a smooth transition into the matter- (dust in this paper) dominated isotropic [Friedmann-Lemaitre-Robertson-Walker (FLRW)] stage. The existence of the background shear causes the mixing of the scalar (density), the vector (rotation), and the tensor (gravitational wave) perturbation modes. Such a coupling smoothly disappears as the background evolution approaches an isotropic stage where the background shear terms vanish. Thus, if we had an anisotropic expansion stage preceding the isotropic stage, we expect the generated tensor mode should be correlated with the scalar mode.

Let us briefly compare the behavior of the perturbations between the radiation and the dust era in the FLRW stage. We consider the density perturbation in the comoving gauge. The comoving gauge completely fixes the temporal gauge transformation. Thus the resulting variables in the comoving gauge are equivalently gauge invariant; see Sec. III of [1]. On scales larger than the visual horizon size, the perturbations in both cases behave similarly. For the scalar mode we have one growing and one decaying mode for δ, whereas for the tensor mode we have one constant mode and one decaying mode. Only the temporal evolution depends on the equation of state. However, inside the visual horizon the behavior of the density perturbations is different considerably depending on the equation of state. For the dust fluid δ behaves in the same way as the case where the perturbation scale is larger than the visual horizon scale. However, for a radiation medium δ starts to oscillate with a constant amplitude. For δ in the comoving gauge, the only scale appearing in the equation is the Jeans scale which is the sound velocity (c_s) times the gravitational time scale $1/\sqrt{G\mu}$. For the dust fluid we have a vanishing sound velocity, thus $c_s = 0$, whereas for the radiation fluid $c_s = c/\sqrt{3}$, thus, comparable to the speed of light. Meanwhile, for the gravitational wave only the visual horizon scale appears in the equation. Thus, for both equations of states, inside the visual horizon, the gravitational wave shows the oscillation with a decaying amplitude.

In the perturbed anisotropic universe the transition time from shear to matter domination appears as an additional scale. In a shear-dominated medium the scalar mode couples with the tensor mode. Thus, inside the horizon and also in a shear-dominated era we expect the mixed tendency between the growing scalar mode and the oscillating tensor mode. Our result shows that the density perturbation inside the horizon oscillates with a decreasing amplitude; see Fig. 6(a).

In this paper we numerically investigate the coupled evolution of the density mode and the gravitational wave through the anisotropic model. For the case of dust filled medium, the perturbation on the Bianchi type-I model has been previously investigated; see [4–6,8]. In [4,7,8] the synchronous gauge condition was used. As will be mentioned in Sec. II C, in a dust fluid the synchronous gauge coincides with the comoving gauge. In [6] a covariant approach was used which in fact corresponds to our comoving gauge analysis in this paper; see Appendix B.

In Sec. II we present the background evolution. The perturbation equations and available exact solutions in the comoving gauge are given. In Sec. III we describe the asymptotic solutions and the numerical method. The results in some

parameter space are presented using the asymptotic solutions in the shear-dominated era. Finally, in Sec. IV we give a brief discussion. As a unit we set $c\equiv 1$.

II. EQUATIONS

We follow the notation introduced in Sec. II B of [2]. In [2] an ideal fluid case was considered. Also, the perturbed set of equations without fixing the temporal gauge was presented in terms of nondimensionalized variables. The dust medium is a pressureless limit of an ideal fluid, thus $w=0$.

A. Background evolution

The background equations are [we let $w=0$ in Eqs. (2)–(4) of [2]]

$$\dot{\mu}+3\dot{s}\mu=0, \quad \ddot{s}_\alpha+3\dot{s}\dot{s}_\alpha=0, \quad \dot{s}^2=\frac{8\pi G\mu}{3}+\frac{1}{6}\sum_\alpha \dot{s}_\alpha^2, \quad (1)$$

where $w\equiv p/\mu$, $s\equiv s(t)$, $s_\alpha\equiv s_\alpha(t)$, and $\alpha=1,2,3$. An overdot denotes the derivative with respect to the background proper time t. From Eq. (A6) of [2] we have

$$e^s=\left[\frac{t(t+2t_s)}{3t_s^2}\right]^{1/3}, \quad e^{s_\alpha}=\left(\frac{t}{t+2t_s}\right)^{S_\alpha/3}, \quad (2)$$

where

$$t_s\equiv\frac{\sqrt{\frac{1}{6}\Sigma_\alpha\dot{s}_\alpha^2}}{4\pi G\mu}, \quad S_\alpha\equiv\frac{\dot{s}_\alpha}{\sqrt{\frac{1}{6}\sum_\beta \dot{s}_\beta^2}}=\frac{\dot{s}_\alpha}{4\pi G\mu t_s}. \quad (3)$$

We normalize $a(t)\equiv e^{s(t)}$ so that $a=0$ at $t=0$. We also set $18\pi G\mu e^{3s}\equiv t_s^{-2}$ and, thus, normalize $a=1$ at t_s. The t_s indicates the transition time from the shear-dominated era into the dust-dominated era. In the limit of shear-dominated era (SDE) and matter- (dust in this case) dominated era (MDE) we have

$$\text{SDE:} \quad t\ll t_s(\eta\propto t^{2/3}): \quad e^s\propto t^{1/3}\propto\eta^{1/2}, \quad e^{s_\alpha}\propto t^{S_\alpha/3}\propto\eta^{S_\alpha/2},$$

$$\text{MDE:} \quad t\gg t_s(\eta\propto t^{1/3}): \quad e^s\propto t^{2/3}\propto\eta^2, \quad e^{s_\alpha}\to 1, \quad (4)$$

where $d\eta\equiv a^{-1}dt$. We present a typical evolution of the background model in Fig. 1.

B. Perturbation wave vector

As in [2] and [3], we *consider* the case where the perturbation wave vector k_α lies in a plane of two principal axes. Thus we assume that a given scale is fixed by a wave vector $k_\alpha=(0,k_2,k_3)$ which is time independent. We consider that the index of k^α is raised by $\gamma^{\alpha\beta}$ which is the background three space metric subtracting the averaged background expansion; see Eq. (1) in [1]. Because of the dependence on background anisotropy of $\gamma_{\alpha\beta}$, k^α depends on time. We have

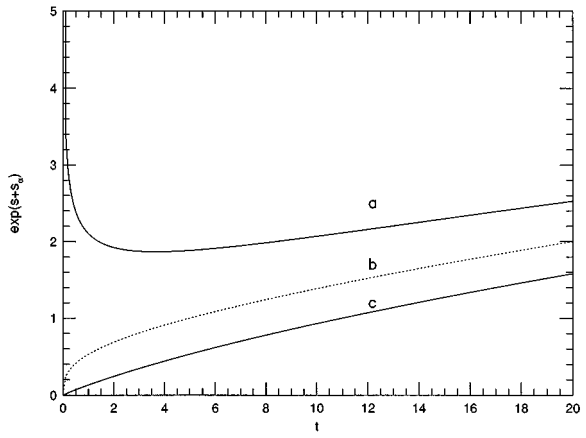

FIG. 1. (a)–(c) represent $e^{s+s_\alpha}(t)$ for $S_\alpha=(-\sqrt{3},0,\sqrt{3})$. In the early stage, the background evolves differently in different direction. But they evolve like the FLRW universe at large t. The transition occurs near $t_s=5$.

$$k^2k_2=\gamma^{22}(k_2)^2=e^{-2s_2}(k_2)^2=\left(\frac{t}{t+2t_s}\right)^{-\frac{2}{3}S_2}(k_2)^2,$$

$$k^3k_3=\left(\frac{t}{t+2t_s}\right)^{-\frac{2}{3}S_3}(k_3)^2. \quad (5)$$

We introduce

$$r\equiv\frac{k_2}{k_3}, \quad \Delta\equiv\gamma^{\alpha\beta}\partial_\alpha\partial_\beta\equiv\nabla^{(3)\alpha}\partial_\alpha. \quad (6)$$

Thus, using $k\equiv\sqrt{k^\alpha k_\alpha}$, we have [see Eq. (A2)]

$$\begin{aligned}\overline{\Delta}&\equiv-\left(\frac{k}{a\dot{s}}\right)^2\\&=-\frac{9}{4}\left(\frac{3t^2t_s^2}{t+2t_s}\right)^{2/3}\left(\frac{t+2t_s}{t+t_s}\right)^2(k_3)^2\left[\left(\frac{t}{t+2t_s}\right)^{-\frac{2}{3}S_3}+\left(\frac{t}{t+2t_s}\right)^{-\frac{2}{3}S_2}r^2\right]. \quad (7)\end{aligned}$$

The horizon crossing epoch of a given scale k, $t_H(k)$, is *defined* as

$$1\equiv\sqrt{-\overline{\Delta}|_H}=\left.\frac{k}{a\dot{s}}\right|_H. \quad (8)$$

From this relation we can express k_3 in terms of t_H and r as

$$k_3=\frac{2}{3}\left(\frac{3t^2t_s^2}{t+2t_s}\right)^{-1/3}\frac{t+t_s}{t+2t_s}\left[\left(\frac{t}{t+2t_s}\right)^{-\frac{2}{3}S_3}+\left(\frac{t}{t+2t_s}\right)^{-\frac{2}{3}S_2}r^2\right]^{-1/2}\Bigg|_{t=t_H}. \quad (9)$$

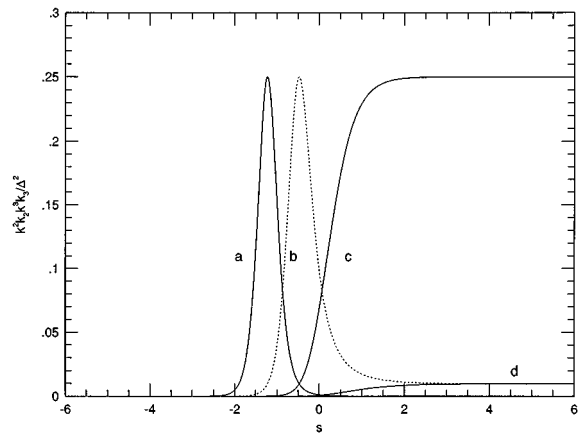

FIG. 2. The time evolution of $k^2k_2k^3k_3/\Delta^2$ for $r=100$ (a), 10 (b), 1 (c), and 0.1 (d). We use $S_\alpha=(0,-\sqrt{3},\sqrt{3})$ and $s_H=19.2$, where s_H is the value of s at the horizon crossing.

The wave vector of the perturbation k_α is characterized by r and t_H; r determines the direction of the perturbation, and t_H determines the size of the perturbation using the horizon crossing epoch of the scale. We present a typical evolution of a combination of the wave vector in Fig. 2.

C. Perturbation equations in the comoving gauge

In [3] a set of perturbation equations in the comoving gauge is presented for a general $w=$const; see Eqs. (14)–(17) of [3]. The equations for a general $w=p/\mu$ without fixing the temporal gauge (thus, in a gauge ready form) are presented in Eqs. (17)–(29) of [2]. For a dust filled medium, we let $w=0$. We ignore the rotation mode, thus $Q_v=0$. In such a case we have $A=0$ and $\delta\bar{K}=\delta'$. The equations become

$$\delta''+\left(2+\frac{\ddot{s}}{\dot{s}^2}-\frac{\Delta'}{\Delta}\right)\delta'-\frac{4\pi G\mu}{\dot{s}^2}\,\delta =\left(s_1'-\frac{\Delta'}{4\Delta}\right)\left(4G'-3\frac{\Delta'}{\Delta}G\right) +4(s_2'-s_3')^2\frac{k^2k_2k^3k_3}{\Delta^2}G -\left[\frac{9}{8}\frac{\Delta'^2}{\Delta^2}+6(s_2'-s_3')^2\frac{k^2k_2k^3k_3}{\Delta^2}\right]C, \tag{10}$$

$$G''+\left(3+\frac{\ddot{s}}{\dot{s}^2}\right)G'-\left[\bar{\Delta}-2(s_2'-s_3')^2\frac{k^2k_2k^3k_3}{\Delta^2}\right]G =\left(s_1'-\frac{\Delta'}{4\Delta}\right)\delta'+3(s_2'-s_3')^2\frac{k^2k_2k^3k_3}{\Delta^2}C, \tag{11}$$

where

$$C=-\left[2\bar{\Delta}-\frac{9\Delta'^2}{8\Delta^2}-6(s_2'-s_3')^2\frac{k^2k_2k^3k_3}{\Delta^2}\right]^{-1}\left\{\left(4+\frac{\Delta'}{\Delta}\right)\delta\bar{K} +\frac{16\pi G\mu}{\dot{s}^2}\,\delta+\left(s_1'-\frac{\Delta'}{4\Delta}\right)\left(4G'-3\frac{\Delta'}{\Delta}G\right) +4(s_2'-s_3')^2\frac{k^2k_2k^3k_3}{\Delta^2}G\right\}. \tag{12}$$

A prime denotes the derivative with respect to s; $'\equiv\partial/\partial s$. The coefficients are determined by the background evolution and the wave vector. For convenience we present the evolution of these coefficients in Appendix A. The equation for the decoupled gravitational wave will be considered in Sec. II D.

For a dust medium without rotation, from Eq. (19) of [2] we have $A=0$ which coincides with the synchronous gauge condition. Thus, in this case, the comoving gauge can be considered as a case of the synchronous gauge with the gauge mode completely fixed. The authors of [4] and [8] took the synchronous gauge condition to investigate the evolution of the perturbation for a dust medium. In the synchronous gauge, from Eq. (19) of [2] we have nonvanishing $\bar{Q}$ which is the remnant gauge mode.

1. Perturbations along a principal axis

For $k_2=0$ the perturbations are directed along one principal axis, $\hat{x}^3$, of the background anisotropy. We may call it the axially symmetric perturbations. We have $\Delta'/\Delta=-2s_3'$; see Eqs. (A1) and (A2). Then, Eqs. (10)–(12) become

$$\delta''+\left(2+\frac{\ddot{s}}{\dot{s}^2}+4s_3'\frac{\frac{2}{9}\bar{\Delta}-s_3'}{\frac{4}{9}\bar{\Delta}-s_3'^2}\right)\delta'-\frac{4\pi G\mu}{\dot{s}^2}\,\frac{\frac{4}{9}\bar{\Delta}+3s_3'^2}{\frac{4}{9}\bar{\Delta}-s_3'^2}\,\delta =(s_1'-s_2')\frac{\frac{4}{9}\bar{\Delta}}{\frac{4}{9}\bar{\Delta}-s_3'^2}(2G'+3s_3'G), \tag{13}$$

$$G''+\left(3+\frac{\ddot{s}}{\dot{s}^2}\right)G'-\bar{\Delta}G=\frac{1}{2}(s_1'-s_2')\delta'. \tag{14}$$

These equations were first derived in [4]; see their Eqs. (5.4) and (5.5). Comparing with the notation of [4] we have $G=\frac{1}{2}\eta$, $t_s=\frac{1}{2}t_b$, and $\dot{s}^2\bar{\Delta}=-FK^2$. If the background anisotropy is symmetric with respect to $\hat{x}^3$ axis, thus $s_1=s_2$, the scalar mode decouples from the tensor mode. This situation will be considered in the next subsection.

2. Exact solutions in the axisymmetric situation

Consider an axisymmetric perturbation along a principal axis of the background which is symmetric around it, thus $k_\alpha=(0,0,k_3)$ and $s_1=s_2$. Equations (13) and (14) show that the scalar mode decouples from the tensor mode. In this case, Eqs. (13) and (14) expressed in terms of t are

$$\ddot{\delta}+2\left(\dot{s}+\dot{s}_3\frac{e^{-2s}\Delta-\frac{3}{2}\dot{s}\dot{s}_3}{e^{-2s}\Delta-\frac{9}{4}\dot{s}_3^2}\right)\dot{\delta}-4\pi G\mu \times\left(1+\frac{9\dot{s}_3^2}{e^{-2s}\Delta-\frac{9}{4}\dot{s}_3^2}\right)\delta=0, \tag{15}$$

$$\ddot{\bar{G}}+3\dot{s}\dot{\bar{G}}-\dot{s}^2\overline{\Delta}\bar{G}=0. \tag{16}$$

An exact solution for the density perturbation was derived in [4]. For $S_1=S_2$ we have two cases with $S_3=\pm 2$. For $S_3=2$ we have

$$\delta(\mathbf{x},t)=\left[\frac{3t_s}{t+2t_s}-\frac{9}{10}\frac{(t+2t_s)^{5/3}(\sqrt{3}t_s)^{4/3}}{t}\partial_3^2\right]c(\mathbf{x}) -\frac{3}{2}\frac{(\sqrt{3}t_s)^{4/3}}{t}\partial_3^2 d(\mathbf{x}),$$

$$C(\mathbf{x},t)=\frac{2t}{t+2t_s}c(\mathbf{x}). \tag{17}$$

For $S_3=-2$ we have

$$\delta(\mathbf{x},t)=\left[3\frac{t_s}{t}-\frac{9}{10}\frac{t^{5/3}(\sqrt{3}t_s)^{4/3}}{t+2t_s}\partial_3^2\right]c(\mathbf{x}) -\frac{3}{2}\frac{(\sqrt{3}t_s)^{4/3}}{t+2t_s}\partial_3^2 d(\mathbf{x}),$$

$$C(\mathbf{x},t)=2\frac{t+2t_s}{t}c(\mathbf{x}), \tag{18}$$

where $c(\mathbf{x})$ and $d(\mathbf{x})$ are the integration constants. In Eqs. (17) and (18) the dominating decaying mode for $C(\mathbf{x},t)$ has vanished.

We note that from these solutions we can derive the solutions for the rest of variables in the same gauge. Also, using the gauge transformation, in principle, we can derive the solutions in other gauge conditions; see Appendix C of [1].

The equation for the gravitational wave in Eq. (16) can be expressed in terms of k_3 and t_s in Eqs. (2) and (7):

$$\ddot{\bar{G}}+2\frac{t+t_s}{t(t+2t_s)}\dot{\bar{G}}-3^{2/3}\left(\frac{t_s}{t}\right)^{4/3}\left(\frac{t}{t+2t_s}\right)^{\frac{2}{3}(1-S_3)}\partial_3^2\bar{G}=0. \tag{19}$$

In FLRW limit, the exact solutions of Eq. (19) are given in Appendix G4 of [1].

D. Decoupled gravitational wave mode

One polarization state of the gravitational wave mode decouples from the coupled mode considered above. The equations are presented in Eqs. (27)–(29) of [2]. Ignoring the vector mode, thus $\bar{Q}_v=0$, we have

$$\bar{G}''+\left[3+\frac{\ddot{s}}{\dot{s}^2}+2(s_1'-s_2')+2(s_2'-s_3')\frac{k^2k_2}{\Delta}\right]\bar{G}' +\left[-\bar{\Delta}+4(s_2'-s_3')(s_1'-s_2')\frac{k^2k_2}{\Delta} +4(s_2'-s_3')^2\frac{k^2k_2k^3k_3}{\Delta^2}\right]\bar{G}=0. \tag{20}$$

The coefficients based on the background and the wave vector evolution are presented in Appendix A.

III. NUMERICAL INVESTIGATION

A. Initial conditions

For a numerical study, we need initial conditions which can be obtained from the asymptotic solutions in the early shear-dominated stage. These asymptotic solutions for a general constant w are derived in Sec. III of [2]. For $w=0$, we have

$$\delta(\mathbf{x},t)\equiv a_1(\mathbf{x})e^{-3s}+a_2(\mathbf{x}) +\overline{\Delta}\left[1+\frac{3}{8(2-S_3)^2(11-4S_3)}\overline{\Delta}\right]a_3(\mathbf{x})+s\overline{\Delta}a_4(\mathbf{x}), \tag{21}$$

$$C(\mathbf{x},t)=-\frac{1}{3}(2-S_3)a_1e^{-3s}-\left[(2-S_3)(7-2S_3) +\frac{3}{4(2-S_3)}\overline{\Delta}\right]a_3-\frac{1}{2}[11-4S_3 +2(2-S_3)(7-2S_3)s]a_4, \tag{22}$$

$$G(\mathbf{x},t)=-\frac{1}{6}(S_1-S_2)a_1e^{-3s}+\left[-\frac{3}{2}\frac{S_3}{S_1-S_2}(2-S_3) \times(7-2S_3)+\frac{3}{8(S_1-S_2)(2-S_3)}(8-7S_3)\overline{\Delta}\right]a_3 +\frac{1}{2}\frac{1}{S_1-S_2}\left[4(7-2S_3)+\frac{1}{2}S_3(-61+20S_3) -3S_3(2-S_3)(7-2S_3)s\right]a_4, \tag{23}$$

where $a_1(\mathbf{x})$, $a_2(\mathbf{x})$, $a_3(\mathbf{x})$, and $a_4(\mathbf{x})$ are four integration constants. The $a_i(\mathbf{x})s$ determine the initial amplitudes of four different modes. For C and G, the dominant a_2 modes have vanished.

For the decoupled gravitational wave $\bar{G}$, the asymptotic solution is obtained from Eq. (20) as

$$\bar{G}(\mathbf{x},t)=g_1(\mathbf{x})e^{-2(S_1-S_2)s}+g_2(\mathbf{x}), \tag{24}$$

where $g_1(\mathbf{x})$ and $g_2(\mathbf{x})$ are the constant coefficients.

B. Parameter space

As explained in [2], the scale and the configuration of the perturbation are specified by the following parameters.

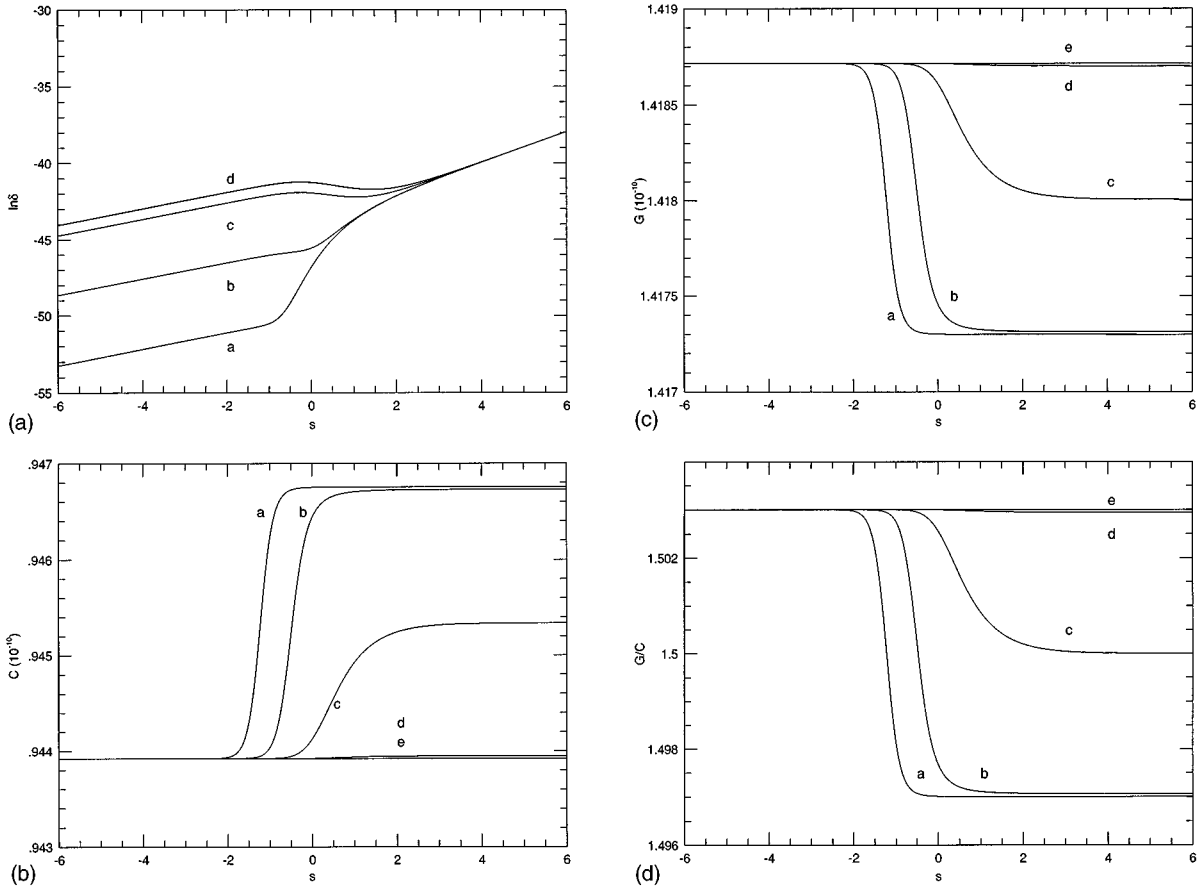

FIG. 3. (a) $\ln\delta(s)$ for $r=0$, 0.01, 0.1 (d), 1 (c), 10 (b), and 100 (a). We take one of the growing mode a_3 as an initial condition. We consider $S_\alpha=(0,-\sqrt{3},\sqrt{3})$. (b) $C(s)$ in the unit of 10^{-10} for $r=0$, 0.01 (e), 0.1 (d), 1 (c), 10 (b), and 100 (a), using $S_\alpha=(0,-\sqrt{3},\sqrt{3})$. The a_3 mode is considered. (c) $G(s)$ in the unit of 10^{-10} for $r=0,0.01$ (e), 0.1 (d), 1 (c), 10 (b), and 100 (a), using $S_\alpha=(0,-\sqrt{3},\sqrt{3})$. The a_3 mode is considered. (d) The ratio of $G(s)$ to $C(s)$ for $r=0$, 0.01 (e), 0.1 (d), 1 (c), 10 (b), and 100 (a), using a_3 mode. We use $S_\alpha=(0,-\sqrt{3},\sqrt{3})$.

(1) $r(\equiv k_2/k_3)$ determines the direction of the perturbation wave vector with respect to the principal axes of the background anisotropy.

(2) η_H or s_H determines the size of the perturbation for given k_3 and r.

(3) S_α determines the rate of the background anisotropy. As shown in Sec. II E of [2], S_α can be parametrized by using u.

For details on this parameter space, see Sec. II E of [2].

C. Numerical method

The evolutions of δ, G, and C were obtained by solving the set of differential Eqs. (10)–(12). The evolution of $\bar{G}$ was obtained by solving Eq. (20). As in the case of the radiation-filled medium, we used the Runge-Kutta method to solve the perturbation equations. For the integration, we fixed the values of r, s_H, and u. We usually set $s_H=19$, unless we consider the small scale perturbations. Since r and u are the important parameters which affect the results, we obtained the results varying these values. We set $s_s=0$, where s_s is the value of s at the transition from the shear-dominated into the dust-dominated era. We usually took the 5000 grid points which are equally divided in time duration, and checked whether our results are sensitive to this resolution or not. For the initial condition, we usually considered the a_3 mode which is the growing mode. For initial amplitudes, we used $a_i=10^{-10}(i=1,2,3,4)$.

D. Results

We show the evolution of δ for different values of r in Fig. 3(a).

As in the case of radiation-filled medium treated in [3], the growth rate of δ changes near the transition time $s_s(=0)$ from the shear-dominated into the dust-dominated era. In the shear-dominated era, δ evolves like $e^{4-2S_\alpha(\mathbf{k}_{\rm eff})}$, where $S_\alpha(\mathbf{k}_{\rm eff})$ indicates the S_α in the direction $\mathbf{k}_{\rm eff}=(0,\sqrt{k^2k_2},\sqrt{k^3k_3})$ effectively. At large value of s, δ evolves like the FLRW case in the dust-dominated era: $\delta\propto e^s$. We see that in the early shear-dominated stage, the background anisotropy strongly affects the evolution of the perturbation.

For large value of r, another change in the growth rate of δ appears between the shear-dominated era and FLRW era. The effective wave vector of the perturbation $\mathbf{k}_{\rm eff}=(0,\sqrt{k^2k_2},\sqrt{k^3k_3})$ changes from $(0,0,\sqrt{k^3k_3})$ into $(0,r\sqrt{k^3k_3},\sqrt{k^3k_3})$. Therefore, for $S_3>S_2$ and large r, $\hat{\mathbf{k}}_{\rm eff}$ effectively changes from $\hat{\mathbf{x}}_3$ into $\hat{\mathbf{x}}_2$. We see that as r increases, the growth rate changes at the earlier time. This can

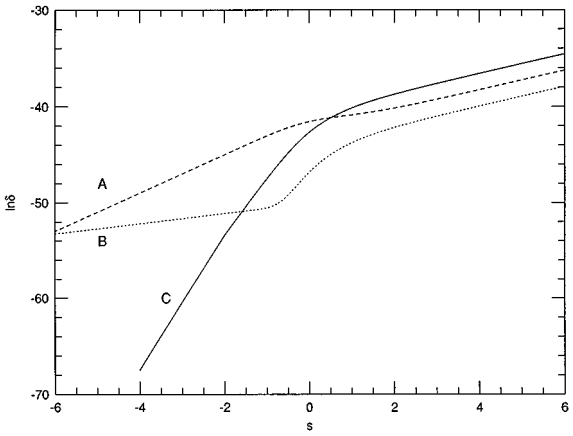

FIG. 4. $\ln\delta(s)$ for three cases: (a) $S_\alpha=(-2,1,1)$, (b) $S_\alpha=(0,-\sqrt{3},\sqrt{3})$, and (c) $S_\alpha=(2,-1,-1)$. We consider $r=100$ and the a_3 mode.

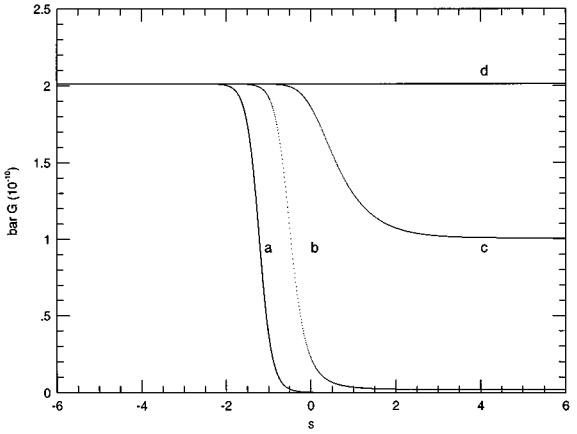

FIG. 5. The evolution of the decoupled gravitational wave $\bar{G}$ in the unit of 10^{-10} for $r=0$ (d), 1 (c), 10 (b), 100 (a). We consider the constant mode as an initial condition and use $S_\alpha=(0,-\sqrt{3},\sqrt{3})$.

be explained by the shift of the slope change in $k^2k_2k^3k_3/\Delta^2$ into the earlier time (see Fig. 2).

The other variables C [Fig. 3(b)] and G [Fig. 3(c)] also show the change in growth rate near the transition time s_s. As in the case of δ, the changes in growth rate of C and G occur at earlier time as r increases. As s increases, C and G approach the FLRW universe in which they remain constant. In Fig. 3(d), we show the relation between C and G for different values of r. As in the case of radiation, the value of C turns out to be comparable to that of G. Similar result can be found in [5] where the uniform-curvature gauge with the spatial C gauge was used. In the anisotropic universe the background anisotropy causes the correlation between the tensor perturbation and the scalar perturbation. In an isotropic universe they evolve independently.

In Fig. 4, the evolutions of δ with different cases of the background models are presented. Figure 4 shows that in the early shear-dominated stage, the evolution of the perturbation is determined by the background anisotropy. At $s\ll s_s$, the perturbations evolve like the $\delta\propto e^{4-2S_3}$, because the wave vector effectively lies in $\hat{x}^3$ direction. But for $s\gg s_s$, the perturbations evolve like in the FLRW universe. In the case of (A) and (C) in which the background is axisymmetric with respect to $\hat{x}^1$ axis, the evolutions of the perturbed variables are independent of r.

In Fig. 5, the evolution of the decoupled gravitational wave perturbation $\bar{G}$ is shown for different values of r. As in the case of the coupled gravitational wave, the decoupled gravitational wave changes its slope at earlier time with increasing r. In the FLRW limit, G becomes constant.

So far, we considered the perturbations in the large scale in which the horizon crossing occurs much later than the transition time s_s. It may be interesting to see the behavior of the perturbations in a small scale. In Figs. 6(a)–6(d) we show the evolution of δ, C, and G in a small scale, respectively. In this case, we assumed that the horizon crossing occurs before the transition time s_s. The perturbed variables start oscillations near the horizon crossing. It is noticeable that in an anisotropic universe, like the case of the radiation-filled medium, δ in the dust-filled universe oscillates with a decreasing amplitude because of the coupling with the gravitational wave perturbation. However, as shown in Fig. 6(b), after the transition time s_s, the perturbation approaches to the FLRW universe where $\delta\propto e^s$; in the FLRW limit the density perturbation will be decoupled from the gravitational wave perturbation.

For comparison, in the case of the radiation-filled medium, after s_s the density perturbation continues the oscillation with a constant amplitude (see Fig. 9(a) in [3]).

Also, in the case of small scale perturbation and in the shear dominated era, we found that our numerical solution agrees with the analytic solution derived in [4]: $\delta\propto t^{(1-2s_3)/3}$ [see Eq. (8.2) in [4]].

IV. DISCUSSION

In this work, we studied the evolution of perturbations in a Bianchi type-I universe filled with the dust. The perturbation equations were obtained based on the ''gauge ready'' formulation presented in [1]. We adopted the comoving gauge which is suitable for investigating the density perturbation.

As in the case of the radiation-filled universe studied in [3] the background shows a smooth transition from the shear-dominated anisotropic universe into the dust-dominated isotropic one. The results show that the change in growth rate occurs near the transition time. In the early time in which the shear dominates, the evolution of the perturbation is governed by the anisotropy of the background. Therefore, the growth rate of the perturbation shows the effect of the directional dependence of the background expansion. In the case of an axisymmetric perturbation in a dust-filled anisotropic universe with the wave vector $\mathbf{k}=(0,0,k_3)$, the result can be compared with the previous work in [4]. In [4], the synchronous gauge was adopted which is equivalent to the comoving gauge in a dust medium.

It may be interesting to compare the result of this work with the case of the radiation obtained in [3]. In an isotropic universe, the evolution of density perturbation in a dust-filled universe is independent of the horizon scale. This is because in the case of dust the sound velocity is negligible. Therefore, perturbations in the small scale behave similarly to the case of large scale. No oscillation occurs inside the horizon.

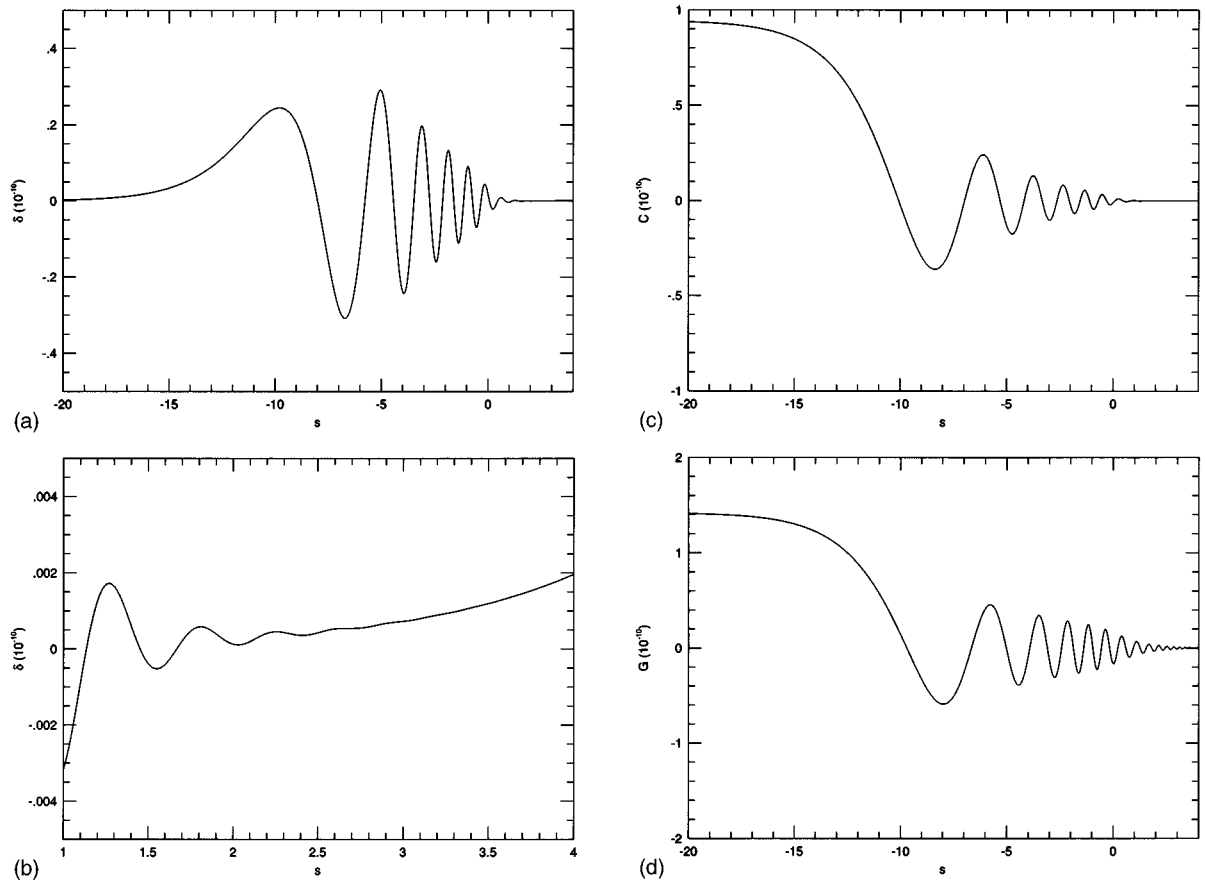

FIG. 6. (a) The evolution of δ in the unit of 10^{-10} using the case where the horizon crossing occurs earlier than the transition time s_s. We set the horizon crossing epoch at $s_H=-8.7$. (b) The evolution of δ in the unit of 10^{-10} after the transition time $s_s=0$. The horizon crossing occurs at $s_H=-8.7$. (c) $C(s)$ in the unit of 10^{-10} using the case where the horizon crossing occurs at $s_H=-8.7$. (d) $G(s)$ in the unit of 10^{-10} using the case where the horizon crossing occurs at $s_H=-8.7$.

While, in a radiation-dominated era, the density perturbation evolves differently depending on whether it is inside or outside the visual horizon. When its wavelength is smaller than the visual horizon, the density perturbation shows the oscillation with a constant amplitude. In the anisotropic universe, the scalar mode perturbation couples with the tensor mode perturbation. Our numerical result shows that inside the horizon, the density perturbation shows the oscillation with a decreasing amplitude because of the coupling with the gravitational wave perturbation.

ACKNOWLEDGMENTS

We thank Dr. J. Hwang for his useful discussions throughout the work. J.H. provided Appendix B.

APPENDIX A: COEFFICIENTS

In the following we present the behavior of background quantities and the wave vector. These terms appear as coefficients of the fundamental perturbation equations in Eqs. (10)–(12), and (20). We have

$$s'_\alpha = S_\alpha \frac{t_s}{t+t_s}, \quad \frac{\ddot{s}}{\dot{s}^2} = -\frac{3}{2}\left[1+\left(\frac{t_s}{t+t_s}\right)^2\right],$$

$$\frac{8\pi G\mu}{3\dot{s}^2} = \frac{t(t+2t_s)}{(t+t_s)^2}. \tag{A1}$$

The evolutions of the wave vector in Sec. II B give

$$\overline{\Delta} = -\left(\frac{t}{t_H}\right)^{4/3}\left(\frac{t+2t_s}{t_H+2t_s}\right)^{4/3}\left(\frac{t_H+t_s}{t+t_s}\right)^2\left(\frac{t}{t+2t_s}\right)^{-\frac{2}{3}S_3} \times\left(\frac{t_H}{t_H+2t_s}\right)^{\frac{2}{3}S_3}\times\frac{1+\left(\frac{t}{t+2t_s}\right)^{\frac{2}{3}(S_3-S_2)}r^2}{1+\left(\frac{t_H}{t_H+2t_s}\right)^{\frac{2}{3}(S_3-S_2)}r^2},$$

$$\frac{\Delta'}{\Delta} = -2\frac{t_s}{t+t_s}\,\frac{S_3+S_2\left(\frac{t}{t+2t_s}\right)^{\frac{2}{3}(S_3-S_2)}r^2}{1+\left(\frac{t}{t+2t_s}\right)^{\frac{2}{3}(S_3-S_2)}r^2},$$

$$\frac{k^3 k_3}{\Delta} = -\frac{1}{1+\left(\frac{t}{t+2t_s}\right)^{\frac{2}{3}(S_3-S_2)} r^2},$$

$$\frac{k^2 k_2}{\Delta} = -\frac{r^2}{\left(\frac{t}{t+2t_s}\right)^{\frac{2}{3}(S_2-S_3)} + r^2}. \tag{A2}$$

APPENDIX B: COVARIANT DENSITY GRADIENT VARIABLE

In a perturbed FLRW model, the authors of [9] introduced a density gradient variable which is covariant and gauge invariant; an application to the anisotropic model was made in [6]. In the perturbation analysis the variable corresponds to a combination of a scalar mode (a gauge invariant combination of the density variable based on the comoving gauge) and a vector (rotational) mode. The variable was generalized into a frame invariant form in [10]. In the following we present a corresponding variable in the general background of Bianchi type-I model.

In Sec. 2.1 of [10] an observer-independent form of the four vector is introduced as

$$u_a^E \equiv u_a + \frac{q_a}{\mu+p}. \tag{B1}$$

The u_a^E is frame independent in the sense that in the energy frame we let $q_a \equiv 0$ whereas in the normal frame we let $u_a \equiv n_a$ where $n_\alpha \equiv 0$. The covariant formulations of the perturbed models in [9,6] are based on the energy frame, whereas the Arnowitt-Deser-Misner (ADM) approach of the slicing the spacetime is based on introducing the normal frame vector. Since we have a freedom in choosing the velocity of the observer, any approach loses no generality. However, by using u_a^E in Eq. (B1) we can have frame-invariant expressions; we put a superscript E in a sense that u_a^E becomes u_a in the energy frame.

Now, we introduce a covariant density gradient variable

$$D_a \equiv \frac{1}{\mu} h^{Eb}{}_a \mu_{,b}, \tag{B2}$$

where μ is the density variable and h_{ab}^E is the projection tensor based on u_a^E: $h_{ab}^E \equiv g_{ab} + u_a^E u_b^E$ (see Sec. 2.1 of [10]). In [1] we derived the equations based on the ADM formulation. The notation used in ADM formulation is slightly different from the covariant notation; see Eq. (E5) of [1] for the correspondences between the fluid quantities, and we used a notation P_{ab} for the projection tensor. Thus, in the ADM notation we have $\mu \to E$ and $q_\alpha \to J_\alpha$; see Eq. (E5) of [1]. The perturbative expansion of the fluid quantities can be found in Eqs. (1) and (4) of [1]. Since in the ADM formulation u_a becomes n_a with $n_\alpha = 0$, in our general frame we need to introduce a general u_α. We let

$$u^\alpha \equiv e^{-s} V^\alpha, \quad u_\alpha = e^s (B_\alpha + V_\alpha), \quad u^0 = e^{-s}(1-A),$$

$$u_0 = -e^s (1+A), \tag{B3}$$

where V^α is based on $\gamma_{\alpha\beta}$. u_a in Eq. (B3) can be compared with n_a in Eqs. (A2) and (3) of [1]; in the normal frame we notice that $B_\alpha + V_\alpha = 0$. Thus, in combination with Eqs. (E5) and (4) of [1], Eq. (B3) becomes

$$u_\alpha^E = e^s \left(B_\alpha + V_\alpha + \frac{Q_\alpha}{\mu+p} \right). \tag{B4}$$

Thus

$$D_\alpha = \frac{1}{\mu}\left[\varepsilon_{,\alpha} + \mu_{,0}\left(B_\alpha + V_\alpha + \frac{Q_\alpha}{\mu+p} \right) \right]. \tag{B5}$$

($D_0 = 0$ because $D_a u_E^a = 0$.) Decomposing V_α into the scalar and the vector mode similarly as in Eq. (12) of [1], thus $V_\alpha \equiv V_{,\alpha} + V_\alpha^{(v)}$, we finally have

$$D_\alpha = \frac{1}{\mu}\left[\varepsilon + \mu_{,0}\left(B + V + \frac{Q}{\mu+p} \right) \right]_{,\alpha} + \frac{\mu_{,0}}{\mu}\left(B_\alpha^{(v)} + V_\alpha^{(v)} + \frac{Q_\alpha^{(v)}}{\mu+p} \right). \tag{B6}$$

In the normal frame, thus $B+V=0$ and $B_\alpha^{(v)} + V_a^{(v)} = 0$, the gauge transformation properties of the complete set of variables are presented in Eqs. (C2)–(C17) of [1]. We notice that only *for* the vanishing background anisotropic pressure, thus $\Pi_{\alpha\beta} = 0$, D_α becomes gauge invariant; see Eqs. (C10), (C12), and (C13) of [1]. In this case we can write

$$D_\alpha = \frac{1}{\mu}(\varepsilon|_Q)_{,\alpha} + \frac{1}{\mu} Q_\alpha^{(v)}. \tag{B7}$$

Thus the scalar part of D_α contains the information about density perturbation based on the comoving gauge; see Eq. (33) of [1].

[1] H. Noh and J. Hwang, Phys. Rev. D **52**, 1970 (1995).
[2] H. Noh and J. Hwang, Phys. Rev. D **52**, 5643 (1995).
[3] H. Noh, Phys. Rev. D **53**, 690 (1996).
[4] T. E. Perko, R. A. Matzner, and L. C. Shepley, Phys. Rev. D **6**, 969 (1972).
[5] K. Tomita and M. Den, Phys. Rev. D **34**, 3570 (1986); M. Den, Prog. Theor. Phys. **77**, 653 (1987); **79**, 1110 (1988).
[6] P. K. S. Dunsby, Phys. Rev. D **48**, 3562 (1993).
[7] P. G. Miedema and W. A. van Leeuwen, Phys. Rev. D **47**, 3151 (1993).
[8] P. G. Miedema, Phys. Rev. D **50**, 2431 (1994).
[9] G. F. R. Ellis and M. Bruni, Phys. Rev. D **40**, 1804 (1989); A. Woszczyna and A. Kulak, Class. Quantum Grav. **6**, 1665 (1989).
[10] J. Hwang, Astrophys. J **380**, 307 (1991).